GEOPHYSICAL RESEARCH LETTERS, VOL. 21, NO. 13, PAGES 1339-1342, JUNE 22, 1994

Multiwavelength lidar observation of thin cirrus at the base of the Pinatubo stratospheric layer during the EASOE campaign

Massimo Del Guasta,[1] Marco Morandi,[1] Leopoldo Stefanutti,[1] Bernhard Stein,[2] Jurgen Kolenda,[2] Patrick Rairoux,[2] J. P. Wolf,[2] Renaud Matthey,[3] and Esko Kyro[4]

Abstract. Multiwavelength lidar measurements carried out in Sodankylä (Finland, 66°N) during EASOE campaign showed high cirrus clouds growing at the base or within Pinatubo aerosol layer. The temperature was generally below -35°C. The mean peak depolarization at 532 nm for all the campaign was 28%, comparable to the values measured in polar cirrus clouds, observed in Dumont d'Urville (Antarctica, 62°S) during 1989, well before the Pinatubo eruption. Optical depth at 532 nm was smaller than 0.3 (thin cirrus). A wavelength dependency was observed in EASOE cirrus backscattering, suggesting a major presence of submicron and micron-sized particles. Such a presence could explain the low depolarization values.

Introduction

Optical and microphysical properties of cirrus growing close to tropopause are poorly known. In situ measurements of smaller particles are scarce or unreliable [Dowling,1990] and modeling of small nonspherical aerosol scattering properties is very complex. As a consequence most models consider such clouds to be composed of big ice crystals (r>10 μm).

Optical properties of polar cirrus are not known on a statistical basis. In this paper cirrus cloud measurements, performed by means of a multiwavelength lidar (355, 532, 750, and 850 nm) during EASOE campaign are presented.

A wavelength dependency of backscattering was observed in several EASOE high cirrus, suggesting clouds dominated by small particles (<2 μm). No definitive indications about the phase, the shape, and the composition of these particles have been retrieved.

Cirrus observed in Sodankylä, during the EASOE campaign, showed lower depolarization ratios than those typically reported for midlatitude cirrus clouds. On the other hand such values are fully comparable with those observed in cirrus clouds at the same latitude, but in the southern hemisphere prior to the Pinatubo eruption. This comparison has been used as a first check of the hypothesis that high cirrus optical properties are modulated by stratospheric aerosols. The presence of a connection between stratospheric particles and ice condensation nuclei is in fact not clear [Mohnen,1990]. The link (if any) should be evidenced after volcanic eruptions due to the enhancement in ice condensation nuclei (volcanic ash) and liquid aerosols concentrations.

No major differences in 532 nm depolarization relation with temperature have been found between Sodankylä (Finland, 66°N) in 1991-92 and Dumont d' Urville (Antarctica, 62°S) in 1989. Nine months after the Pinatubo eruption, the temporal and geographical uniformity of the lidar-measured parameters seems to indicate no dramatic changes in the high polar cloud particle size and shape.

Experimental Setup

The main characteristics of the lidar system [Stefanutti et al. 1992] are now summarized.

Transmitters: a Nd:YAG laser provides both the 355 and the 532 nm wavelength emissions. The pulse energies are 350 mJ at 532 nm and 150 mJ at 355 nm. A tunable Ti:Sapphire laser is used to generate a pair of near IR wavelength emission at 750 and 850 nm. The pulse energies are 350 mJ at 750 nm and 300 mJ at 850 nm. Both laser sources have a 10 Hz maximum repetition rate and the full-angle divergencies are smaller than 1 mrad.

The receiver is a 0.16 m^2 telescope, with a 0.6 mrad full-angle field of view. Two crossed polarization detection channels are used. The acquisition system is based on two 12 bit 5 MHz waveform recorders and a PC for data storage. During EASOE the system has been operated at the Finnish Meteorological Observatory in Sodankylä, from December 1991 to the middle of March 1992. Three PTUW soundings per day, from the same site, were available.

All the four wavelengths have been used to retrieve the stratospheric aerosol particle size distribution, while only the 532 and 750 nm lidar measurements have been used to investigate the cirrus cloud properties.

Lidar Data Inversion

The lidar processing program searches the rawindsonde data closest to the lidar acquisition and computes the molecular density profile. The squared range corrected lidar return is converted into a raw backscattering profile by fitting the signal to the molecular density profile; the fitting region is chosen above the top of the Pinatubo layer. The raw backscattering profile is then corrected for extinction by using Klett algorithm [Klett, 1981]. The atmosphere is assumed to be molecular at the cloud+Pinatubo layer top (r_m). The value $\sigma_R(r_m)$ of the molecular extinction coefficient is used as reference value at the upper edge of the integration interval of Klett's method. The dependence between σ and ß is assumed

[1] I.R.O.E. - C.N.R. Firenze (Italy)
[2] Freie Universitat Berlin (Germany)
[3] Observatoire Cantonal Neuchatel (Switzerland)
[4] Finnish Meteorological Institute Sodankyla (Finland)

Paper number 93GL03077
0094-8534/94/93GL-03077$03.00

of the form: $\beta(z)=K1\sigma(z)^{k2}$. "Standard" backward Klett's method involving only a bound ($\sigma(r_m)$) assumes k2=1. In order to use a variable k2, a second bound has been imposed, arbitrarily assuming a molecular atmosphere below cloud base. The Klett inversion routine is iterated by varying the value of k2, until a good fit between the molecular atmosphere profile and the extinction corrected lidar return is found.

According to results of simulations, the overall relative accuracy of retrieved backscattering and depolarization is estimated to be 20%. The errors derive mainly from neglecting the aerosol loading below the cloud base, from lidar misalignments, and from bad fitting with the molecular atmosphere.

All the data of the EASOE campaign have been processed and the retrieved profiles (i.e. backscattering, extinction and depolarization) archived into a data base. A "cirrus" archive file has been produced for the whole campaign, including all the available lidar and meteorological information at the cirrus characteristic levels such as base, top, mid-cloud altitudes.

Results

Cirrus were observed on 50% of the 56 days of lidar operation in Sodankylä, mostly on February and March. Most of them were detected at tropopause level or just above it (between tropopause and hygrolapse, always). Often cirrus grew within the Pinatubo layer (figure 1). On the other occasions an aerosol gap of several hundred meters was present between the cirrus and the sharp base of the stratospheric layer.

For clouds colder than -50 °C the vertical extension ranged typically between 1000 and 3000 m. Optical depths (computed from 532 nm lidar data, figure 2) were usually smaller than 0.3 (thin cirrus) and often smaller than 0.05 (subvisible cirrus [Sassen, 1989]). Such clouds were generally invisible to the naked eye, also because optical phenomena and precipitation trails were absent. As a consequence of their horizontal homogeneity such cirrus appeared as thin continuous hazy layers.

Cirrus Depolarization.

Peak depolarization values at 532 nm are reported in figure 3, with definition:

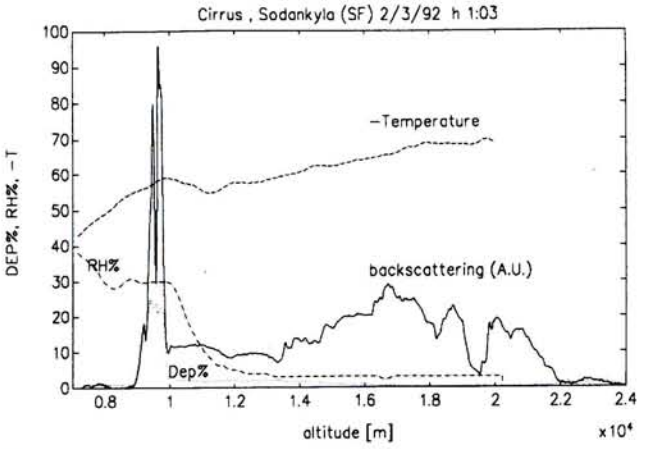

Fig.1: Lidar and radiosonde profiles between 8 and 24 km. A high thin cirrus (corresponding to the depolarization peak) grows at Pinatubo base, inside the aerosol layer and just below tropopause.(Backscattering units are arbitrary).

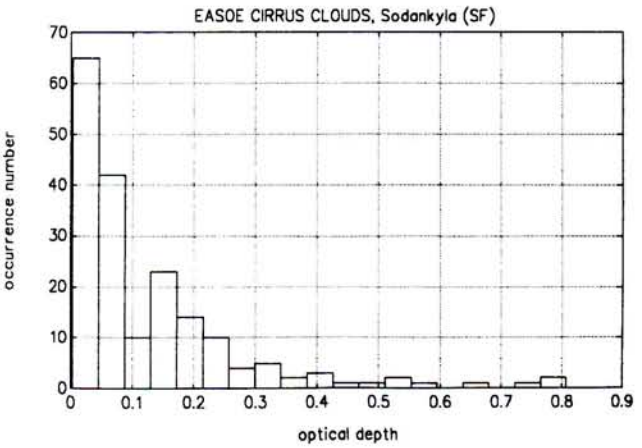

Fig.2: Optical depths of cirrus at 532 nm as estimated by means of lidar data only. Values are generally below 0.2.

$$Dep = \beta_{CS}/\beta_{CP}$$

where β_{CS} is the cloud backscattering of light polarized perpendicularly to laser linear polarization and β_{CP} the Cloud backscattering of light parallel to laser polarization.

The mean peak depolarization at 532 nm for all EASOE cirrus profiles is 28%. No evident differences have been detected between depolarization at 532 and 750 nm.

The depolarization expected for optically thin layers of liquid droplets is below 10%, while ice layers are known to show values between 20 and 80%, with most observations between 40 and 50% [Sassen, 1991]. Lower depolarization have been sometimes observed in ice clouds.

The peak depolarization observed in EASOE cirrus lie at the boundary between ice cloud and water cloud values. Similar figures have been obtained in tropical cirrus [Platt, 1987], in some subvisible cirrus [Sassen, 1989], and in one year of cirrus clouds from Dumont d' Urville [Del Guasta et al., 1992]. A comparison between the latter data and EASOE data is given in figure 3. All DDU cloud data are shown, and can be seen that below about -30°C depolarization is rather constant. Similar temperature relation is visible in EASOE cirrus.

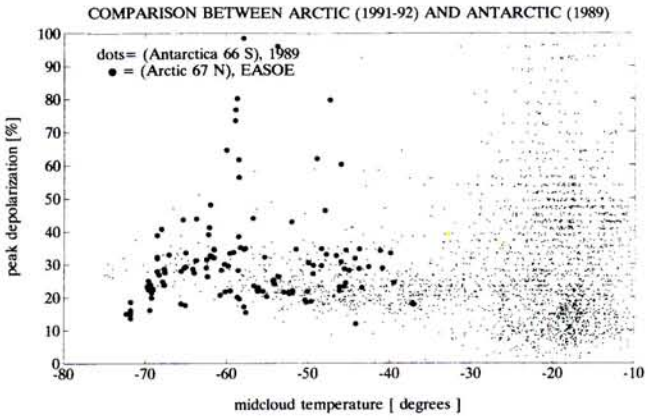

Fig.3: Comparison of EASOE cirrus peak depolarization at 532 nm is performed with one year of Dumont D'Urville (Antarctica) 532 nm lidar cloud data [Del Guasta et al.1992]. Temperature trend below -30°C is similar, despite temporal and geographical differences.

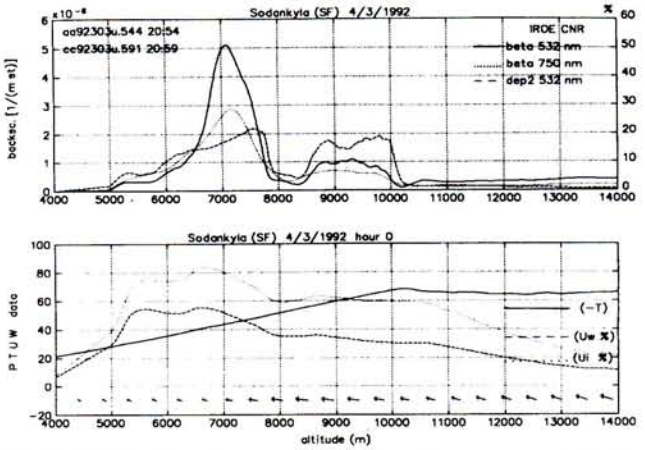

Fig.4: Plot of a two wavelength cirrus measurement: backscattering at 532 and 750 nm is shown, together with depolarization at 532 nm and the closest rawindsounding data: the ratio $ß_{532}/ß_{750}$ is far from unit, suggesting the presence of small particles.

When observed in cirrus, "low" depolarization values are often attributed to the presence of big (>100 μm) horizontally oriented ice plates [Platt, 1978]. The presence of such big plates below -40°C in conditions of water subsaturation (as observed in Sodankylä) is unlikely to occur [Pruppacher e Klett, 1985; Sassen, 1989] and can not explain the common low depolarization measured in cold polar cirrus (figure 3). Moreover, optical phenomena around the sun suggesting the presence of horizontal plates were practically absent in Sodankylä during EASOE campaign.

Another answer to the low depolarization problem could be the presence of liquid droplets and ice particles, together. Supercooled water is short living below -40°C, but, in the presence of enhanced sulfuric aerosols liquid droplets have been detected in cirrus as cold as -50°C [Sassen, 1992]. The presence of low depolarization far below -50°C in EASOE and DDU data (figure 3) could then be explained by a mix of ice particles and sulfuric haze. A similar hypothesis was suggested by [Sassen, 1989] for warmer subvisible cirrus.

Instead of a liquid haze, a frozen one could in principle produce the same depolarization reduction. In this case a theoretical lack arises, because small nonspherical particles are poorly modeled [Asano, 1983] and their contribution to depolarization is still vague.

The occurrence of particles smaller than 10/20 μm in cirrus is not well assessed because of the lack of reliable in-situ probes [Dowling et al, 1990]. Indications of cirrus crystal size decreasing with height and of an important presence of particles smaller than 20 μm are reported only in a few references [g.e. Platt and Spinhirne, 1989], based on in situ and remote sensing measurements.

As a last answer to the problem, it is simply possible that the reported "low" depolarization values are a normal feature of polar cirrus, due to big (r_{eq} >> 1 μm) columnar ice particles only. Columns are supposed to be the most common crystal type at tropopause conditions [Pruppacher et al, 1985], theoretically capable to give 20% depolarization [Yi-Yi Sun et al, 1989] without invoking any haze.

An interesting feature of figure 3 is that DDU clouds at temperature <-30 °C and EASOE cold cirrus show similar depolarization behaviors with temperature, despite geographical differences.

DDU clouds were measured well before Pinatubo eruption, while EASOE followed it. From this first analysis it seems that the stratospheric aerosol enhancement has not dramatically changed cold cirrus depolarization in polar regions.

Wavelength Dependency Of Backscattering In Easoe High Cirrus.

Multiwavelength backscattering lidar and backscattering sondes are capable to give valuable indications on the size of cloud particles. EASOE cirrus clouds have been studied by using 532 and 750 nm lidar data. Such wavelengths were the most powerful of the four available, allowing us to measure clouds with a short integrating time. Expecting a flat wavelength dependency of backscattering coefficient with wavelength in high cirrus (assuming the crystal's equivalent radius to be much larger than wavelength), we instead observed a wavelength dependency (figure 4) that would suggest a major presence of small particles. For several cirrus 532 nm and 750 nm measurements were carried out sequentially. During such time cirrus lidar profile changed with time because of natural fluctuations. By considering only the pairs of measurements taken on uniform cirrus layers within 2-3 minutes time lapse, the ratio between lidar-derived peak backscattering coefficients at 532 and 750 nm was computed, producing the histogram of figure 5. This histogram shows that despite natural changes in lidar profile with time (when changing wavelength), the ratio is always larger than 1.5. This result has been compared with Mie simulation for lognormal distributions of spheres composed of ice (figure 6) or sulfuric acid at different concentrations. For this purpose, scattering efficiencies have been computed with a size parameter resolution dx=0.01. Backscattering coefficient simulations at 532 and 750 nm have been obtained by integrating the efficiencies on lognormal distributions of the form:

$$N(r) = \frac{Nt}{\sqrt{2\pi}\, r \ln(s)} \exp[-0.5(\ln(\frac{r}{rm})/\ln(s))^2]$$

with r_m= median radius, s= width, Nt= total aerosol number.

By varying r_m and s with steps of 0.05 μm and 0.05 respectively and computing the ratio β_{532}/β_{750}, figure 6 is obtained.

When considering ice, (and a minimum value of 1.5 for observed $ß_{532}/ß_{750}$), an upper limit of 1.5 μm for the lognormal

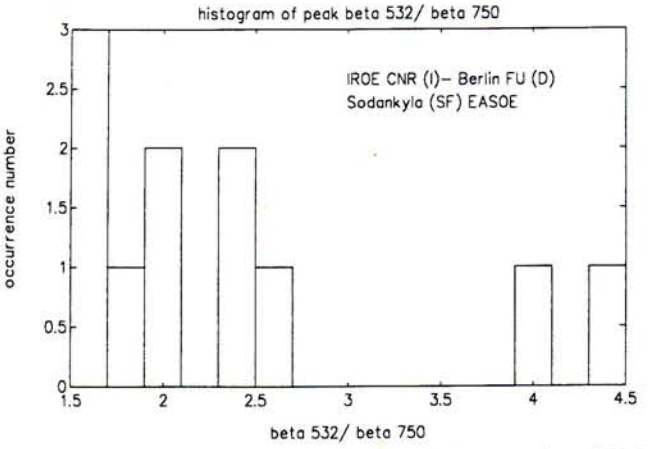

Fig.5: Histogram of $ß_{532}/ß_{750}$ ratio for all closest pairs of 532 and 750 nm measurements of EASOE cirrus. The ratios were larger than about 1.5.

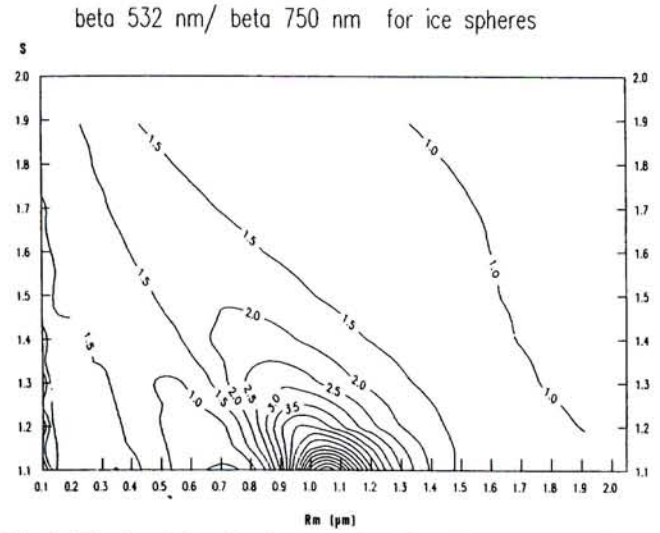

Fig.6: Mie simulation for lognormal radius distributions of ice spheres. X axis is lognormal median radius in [µm], Y axis is distribution width s ([]). (For 70% sulfuric acid (larger refractive indexes) all the plot is shifted toward left). With experimental values $ß_{532}/ß_{750}>1.5$, an equivalent median (and mean) radius <1.5 µm is obtained for ice. 50% sulfuric acid gives r<1.4 µm.

median radius is found for very narrow distributions (s=1.1). When considering s=2 in order to fit real cirrus distributions in the big particles range, a median radius of about 0.4 µm is achieved (mean radius = 0.5 µm). When considering 50% sulfuric acid spheres, the median radius limit is 1.4 µm (s=1.1), becoming 0.3 µm with s=2 (mean radius = 0.4 µm). Distinction between sulfuric aerosols and ice particles is impossible from our data, but in each case the resulting mean radius has the same magnitude.

Mie simulations for spheres have only an indicative value when sizing particles of unknown shape and composition. Anyway, the small mean radius obtained for EASOE high cirrus suggests that most of them were dominated by submicron or micron-sized particles. (A possibility remains that the measured wavelength dependency was merely due to fluctuations of cloud density during the two wavelength measurements, but apart from this no other published explanations are known to the authors which can account for the observed wavelength dependency). This result supports the interpretation of a low polar cirrus depolarization due to the presence of haze particles (frozen or not), suggested in the previous paragraph.

Acknowledgments. We wish to thank the whole staff of Sodankylä Observatory, V.M. Sacco of IROE for the acquisition software, F. Castagnoli and L. Zuccagnoli for the technical project and the building of the instrument. This work was supported by the European communities DG XII under contract STEP CT910141.

References

Asano S., Light scattering by horizontally oriented spheroidal particles, Appl. Optics, 22, No.9, 1390-1396, 1983.

Del Guasta M., M. Morandi, L. Stefanutti, J. Brechet, J. Piquard, One year of cloud lidar data from Dumont d' Urville (Antarctica). Part I: general overview of geometrical and optical properties, *J. Geoph. Res.*, 93, No D10, 1993.

Dowling D.R. and Radke L.F., A summary of physical properties of cirrus clouds, J. of Appl. Meteor., 29, 970-978, 1990.

Klett J. D., Stable analytical inversion solution for processing lidar returns, Applied Optics, 20, No 2, 211-220, 1981.

Morandi M., A complete procedure for inverting backscattering lidar returns. Research Report I.R.O.E. CNR No RR/GCF/92.11, 1992.

Platt C.M.R., Abshire N.L., McNice G.T., Some microphysical properties of an ice cloud from lidar observation of horizontally oriented crystals., J. of Appl. Meteor., 17, 1220-1224, 1978.

Platt C.M.R., Remote sounding of high clouds, part VI:optical properties of midlatitude and tropical cirrus, J. of Atm. Sc., 44, 4, 729-747, 1987.

Platt C.M.R., Spinhirne J.D., Hart W.D., Optical and microphysical properties of a cold cirrus cloud: evidence for regions of small ice particles, J.of Geoph. Res, 94, D8, 11151-11164, 1989.

Pruppacher H.R., Klett D.J., Clouds and precipitation; Reidel publishing company, 1985.

Sassen K., Griffin M.K. and Dodd G.C., Optical scattering and microphysical properties of subvisual cirrus clouds, and climatic implications, J.of Appl. Meteor., 28, 91-98, 1989.

Sassen K., The depolarization lidar technique for cloud research: a review and current assessment, Bull. Am. Meteorol. Soc., 72, 12, 1848-1866, 1991.

Sassen K.,1992, Evidence for liquid-phase cirrus cloud formation from volcanic aerosols: Climatic implications, Science, 257, 516-519, 1992.

Stefanutti L., F.Castagnoli, M.Del Guasta, M.Morandi, V.M.Sacco, V.Venturi, L.Zuccagnoli, J.Kolenda, H.Kneipp, P.Rairoux, B.Stein, D.Weidauer, J.P.Wolf, A four wavelength depolarization backscattering lidar for PSC monitoring, Appl.Phys. B, 55, 13-17, 1992.

Mohnen V.A., Stratospheric Ion and aerosol chemistry and possible links with cirrus cloud microphysics- a critical assesment, J. of the Atm. Sc., 47, 16, 1933-1947, 1990.

YiYi Sun, Zhi-Ping Li, J. Bosenberg, Depolarization of polarized light caused by high altitude clouds. 1: depolarization of lidar induced by cirrus, Appl. Opt., 28, 17, 3625-3639, 1989.

Del Guasta, Morandi, Stefanutti: IROE-CNR via Panciatichi 64, 50127 Firenze, Italy

Stein, Kolenda, Rairoux, Wolf: Institut fur Experimentalphysik, Freie Universitat Berlin, Arnimallee 14, D14195, Berlin-Dahlen, Germany

Matthey, Neuchatel Observatory, Rue de l'Observatoire 58, CH 2000, Neuchatel, Switzerland

Kyro, Finnish Meteorological Observatory, SF-99600, Sodankylä, Finland

Received: November 13, 1992 Revised: March 23, 1993
Accepted: November 1, 1993